J. Cent. South Univ. (2016) 23: 1508−1514
DOI: 10.1007/s11771-016-3202-1

Springer

Improved SMB speckle filtering of polarimetric SAR data with synergistic use of orientation angle compensation and spatial majority rule

LIU Lin(柳林)[1, 2], JIANG Li-ming(江利明)[1], LI Hong-zhong(李洪忠)[3]

1. State Key Laboratory of Geodesy and Earth's Dynamics, Institute of Geodesy and Geophysics, Chinese Academy of Sciences, Wuhan 430077, China;
2. University of Chinese Academy of Sciences, Beijing 100049, China;
3. Shenzhen Key Laboratory of Spatial Information Smart Sensing and Services, Shenzhen University, Shenzhen 518060, China

Abstract: The scattering-model-based (SMB) speckle filtering for polarimetric SAR (PolSAR) data is reasonably effective in preserving dominant scattering mechanisms. However, the efficiency strongly depends on the accuracies of both the decomposition and classification of the scattering properties. In addition, a relatively weak speckle reduction particularly in distributed media was reported in the related literatures. In this work, an improved SMB filtering strategy is proposed considering the aforementioned deficiencies. First, the orientation angle compensation is incorporated into the SMB filtering process to remedy the overestimation of the volume scattering contribution in the Freeman-Durden decomposition. In addition, an algorithm to select the homogenous pixels is developed based on the spatial majority rule for adaptive speckle reduction. We demonstrate the superiority of the proposed methods in terms of scattering property preservation and speckle noise reduction using L-band PolSAR data sets of San Francisco that were acquired by the NASA/JPL airborne SAR (AIRSAR) system.

Key words: scattering-model-based (SMB) speckle filter; polarimetric synthetic aperture radar; orientation angle compensation; spatial majority rule

1 Introduction

Synthetic aperture radar (SAR) is an established active remote-sensing technology that has been widely used in various aspects of earth observation from both airborne and satellite platforms [1]. Polarimetric SAR (PolSAR) uses different radar polarizations for transmitting and receiving antennas to obtain polarimetric characteristics of the imaged terrain targets [2]. Speckle filtering of PolSAR data is essential for better information extraction in various earth science applications, such as geophysical parameter estimation, target detection and terrain classification. However, because the polarimetric signature should be preserved and it is necessary to avoid introducing the cross-talk among polarization channels, speckle filtering is more complicated to implement in the PolSAR product than in a single-polarization SAR data.

Over the last 20 years, several speckle-filtering strategies have been proposed for PolSAR images. Here, the recent advances in PolSAR filtering are briefly reviewed. In the early years, most speckle-filtering methods for multi-polarization or polarimetric SAR data either ignored or improperly filtered the off-diagonal terms of the covariance or coherency matrix [3−5]. Consequently, these filters cannot fully preserve the polarimetric properties because they introduce cross talk among the polarization channels. The recently proposed filters considered these problems. Assuming a stationary and multiplicative noise, LEE et al [6] developed a refined MMSE filter to better preserve the spatial resolution details. GU et al [7] derived the subspace decomposition filter to discard a non-principle component from the local covariance matrix as noise. Based on the concept of the Lee sigma filter and a region-growing technique, VASILE et al [8] proposed a PolSAR speckle-filtering algorithm. CHEN et al [9] introduced the nonlocal filtering algorithm for PolSAR image denoising and showed noticeable improvements in both fine-structure preservation and speckle reduction.

Foundation item: Project(2012CB957702) supported by the National Basic Research Program of China; Projects(41590854, 41431070, 41274024, 41321063) supported by the National Natural Science Foundation of China; Project(Y205771077) supported by the Hundred Talents Program of the Chinese Academy of Sciences
Received date: 2015−03−31; **Accepted date:** 2015−12−10
Corresponding author: JIANG Li-ming, Professor, PhD; Tel: +86−27−86778612; E-mail: jlm@whigg.ac.cn

In general, the basic idea of the speckle-filtering method is to select homogenous pixels of identical statistical properties to include in the filtering process. LEE et al [10] extended this idea to select homogenous pixels of a PolSAR image with identical scattering mechanisms and proposed the so-called scattering-model-based (SMB) filtering method. This new filter (hereafter referred to as Lee's SMB filter) consists of the following three main procedures: 1) compute the Freeman-Durden decomposition, 2) divide pixels into classes by applying the unsupervised classification, which preserves the dominant scattering mechanism, and 3) apply speckle filtering based on the classification map. Because this method exploits the dominating scattering mechanism of each pixel, it is reasonably effective in both scattering characteristic preservation and speckle noise reduction. However, this efficiency strongly depends on the accuracy of both decomposition and classification. It is well known that the fundamental properties of the Freeman-Durden decomposition affect the correct classification of the actual scattering mechanisms of terrain media [11]. This incorrect classification of target scattering characteristics basically results from the emergence of negative power values on some pixels, which is most frequently associated with double-bounce scattering and surface scattering [12]. Moreover, the speckle noise affects the decomposition and classification results and can cause improper selection of homogenous pixels [9, 13], which leads to a relatively weak speckle reduction, particularly in the distributed media [14].

In this work, we developed an improved SMB filtering strategy that overcomes these inherent deficiencies of the Lee's SMB filter. This work is an extension of our previous works, where we used a spatial proximity approach similar to that of LANDGREBE [15] to select homogenous pixels [13], and the Barnes decomposition method for X-band TerraSAR data [11]. First, the orientation angle (OA) compensation of the coherency matrix is introduced into the Freeman-Durden decomposition to reduce the classification errors of scattering properties, which are mainly caused by inherent drawbacks of the model-based decompositions. In addition, the spatial majority rule is proposed in filtering to alleviate the effect of decomposition and classification errors on the homogenous-pixel selection.

2 Drawbacks of Lee's SMB filter

The following two drawbacks have been detected and should be corrected or compensated, according to the basic principle of the Lee's SMB filter.

1) Misclassification of scattering characteristics because of inherent limitations with the model-based polarimetric decompositions: The robust determination of target scattering categories based on the Freeman-Durden decomposition is essential to preserve the dominant scattering mechanism of each pixel in the SMB filtering [10]. However, this decomposition and also its extended version of the four-component decomposition [16] were derived under the assumption of reflection symmetry, which makes the powers of surface scattering or double-bounce scattering occasionally become negative for some pixels. Consequently, these decompositions interpret erroneous scattering characteristics for some terrain targets. In particular, if the buildings are not aligned in the radar look direction, they may not be characterized as double-bounce scattering and are incorrectly categorized as volume scattering because of their higher HV returns. To reduce the number of pixels with negative powers to improve the classification accuracy of the scattering characteristics, the orientation angle shifts must be compensated by rotating the coherency matrix about the line of sight before decomposition.

2) Bias in the homogenous-pixel selection: In Ref. [10], speckle filtering for distributed scatters was to average the homogenous pixels with identical scattering mechanism as the central pixel in a moving window. In the case of a low speckle noise level for the distributed targets, this selection method of homogenous pixels is basically reasonable for the averaging process because the central pixel and its neighbors should theoretically have identical scattering mechanism. However, this selection method is strongly influenced by the aforementioned decomposition and classification errors, particularly when the speckle noise levels are high [9, 13]. The possible worst case occurs when the central pixel is a speckle or when the amplitude level of the central pixel is near the noise level [13]. In this work, following the Freeman-Durden decomposition and the scattering category classification, a simple but robust algorithm based on the spatial majority rule is adopted in filtering to select homogenous pixels that are similar in both scattering mechanism and spatial statistics property.

3 Improved SMB filtering methodology

The improvements of the proposed SMB filtering strategy are mainly highlighted by two key procedures: compensation of the orientation angle shift and selection of the homogenous pixels based on the spatial majority rule. Figure 1 illustrates the general flowchart of the improved SMB filtering strategy. Here, we focus on detailed descriptions of these two key procedures as follows, which alleviates the two main drawbacks of Lee's SMB filter.

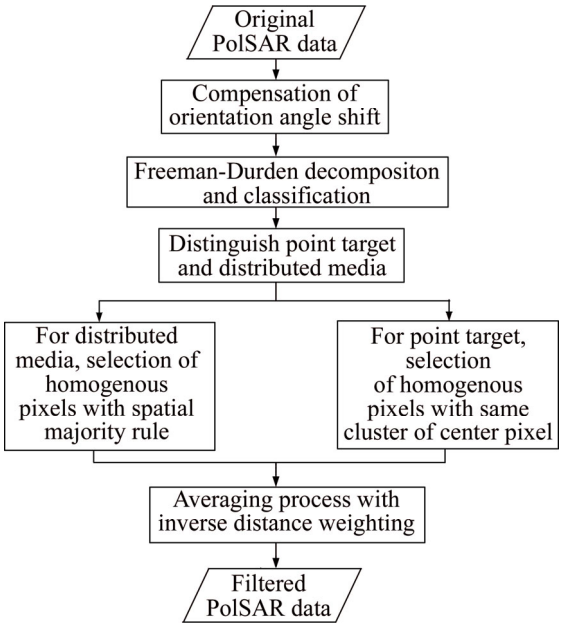

Fig. 1 Processing flowchart of improved SMB filtering strategy

3.1 Compensation of orientation angle shift

Compensation of orientation angle is principally defined as rotating the coherency matrix T about the line of sight to minimize the cross-polarized scattering power (e.g., T_{33} is a component in Eq. (2)). The minimization of the cross-polarized scattering indicates that the OA compensation before applying the scattering-model-based decompositions can reduce the volume power and increase the double-bounce power. Consequently, it is desirable to reduce the number of pixels with negative powers and to suppress the effect of overestimating the volume-scattering power, thus improving the decomposition and classification accuracy of the dominant scattering characteristics.

In this work, we adopted the deorientation algorithm to minimize the cross-polarized power, which was proposed by XU and JIN [17] because it was developed on a sound theoretical basis and is computationally efficient. For each pixel of a PolSAR image, the OA compensation is derived as follows:

$$\boldsymbol{T}^{\theta} = \boldsymbol{U}\boldsymbol{T}\boldsymbol{U}^{\mathrm{H}} \tag{1}$$

with

$$\boldsymbol{T} = \begin{bmatrix} T_{11} & T_{12} & T_{13} \\ T_{12}^{*} & T_{22} & T_{23} \\ T_{13}^{*} & T_{23}^{*} & T_{33} \end{bmatrix} \tag{2}$$

$$\boldsymbol{U} = \begin{bmatrix} 1 & 0 & 0 \\ 0 & \cos(2\theta) & \sin(2\theta) \\ 0 & -\sin(2\theta) & \cos(2\theta) \end{bmatrix} \tag{3}$$

where $\boldsymbol{T}^{\theta}$ and $\boldsymbol{T}$ are the coherency matrixes after and before the rotation by θ, respectively; $\boldsymbol{U}$ is a unitary rotation operator; The superscript H denotes the conjugate transpose. Because $\boldsymbol{U}$ is defined by the sine and cosine of 2θ, the effective range of the orientation angle θ is $(-\pi/2, \pi/2)$.

In terms of the OA compensation, the elements of the coherency matrix are expressed as follows.

$$T_{11}^{\theta} = T_{11} \tag{4}$$

$$T_{22}^{\theta} = T_{22}\cos^2(2\theta) + T_{33}\sin^2(2\theta) + \mathrm{Re}(T_{23})\sin(4\theta) \tag{5}$$

$$T_{33}^{\theta} = T_{33}\cos^2(2\theta) + T_{22}\sin^2(2\theta) - \mathrm{Re}(T_{23})\sin(4\theta) \tag{6}$$

$$T_{12}^{\theta} = T_{12}\cos(2\theta) + T_{13}\sin(2\theta) \tag{7}$$

$$T_{21}^{\theta} = T_{21}\cos(2\theta) + T_{31}\sin(2\theta) \tag{8}$$

$$T_{13}^{\theta} = -T_{12}\sin(2\theta) + T_{13}\cos(2\theta) \tag{9}$$

$$T_{31}^{\theta} = -T_{21}\sin(2\theta) + T_{31}\cos(2\theta) \tag{10}$$

$$T_{23}^{\theta} = \mathrm{j}\,\mathrm{Im}(T_{23}) \tag{11}$$

$$T_{32}^{\theta} = -\mathrm{j}\,\mathrm{Im}(T_{23}) \tag{12}$$

To minimize the T_{33}^{θ}, we must calculate the derivative with respect to θ. The orientation angle is the θ that makes the expression equal zero, and the equation is written as

$$2(T_{22} - T_{33})\sin(4\theta) - 4\,\mathrm{Re}(T_{23})\cos(4\theta) = 0 \tag{13}$$

Therefore, the orientation angle is derived from the following expression:

$$\theta = \frac{1}{4}\tan^{-1}\left(\frac{2\,\mathrm{Re}(T_{23})}{T_{22} - T_{33}}\right) \tag{14}$$

Applying the orientation angle in Eq. (14), all elements of the compensated coherency matrix $\boldsymbol{T}^{\theta}$ can be calculated using Eqs. (4)−(12).

3.2 Selection of homogenous pixels

Considering the previously mentioned drawback in selecting homogenous pixels, a spatial majority voting approach is used to identify the neighboring pixels of a homogenous area that have similar scattering mechanisms and statistics properties. As a popular decision rule, majority voting derives from the statistics hypothesis that the decision of the most prevalent voting (e.g., more than half of the votes) is superior to that of the minority [18]. Because this method is easy to operate, it has been widely used as an ensemble algorithm for multiple classifiers or post-classification processing methods to improve the classification accuracy [19].

In our work, based on the principle of spatial majority voting, the pixels of the prevalent scattering class with the largest number of pixels in a window are selected as homogenous pixels to filter the central pixel.

If there is more than one prevalent scattering class in the same category, all pixels that correspond to these prevalent classes are used in the majority filtering. Moreover, inverse distance weighting (IDW) is applied in the weighted averaging process of those identified homogenous pixels because the pixels closer to the central pixel should have more similar clustering property. For the distributed media, the use of spatial majority rule indicates that the effect of the decomposition and classification errors may be greatly alleviated using the more robust selection of homogenous samples. Thus, compared to the selection method of LEE et al [10], this method provides a relatively high performance of polarimetric properties preservation and speckle reduction. A mathematical model of the weighted average of those homogenous pixels that correspond to the majority class is described as follows: in the defined moving window, the majority class ω_{m} can be determined by counting the number of pixels for each class, which is derived based on the Freemen-Durden decomposition and the Wishart classifier; then, the central pixel value is assigned by

$$I_{(x.y)}=\sum_{i}^{n} w_i I_{(x_i y_i)} \tag{15}$$

where $I_{(x_i y_i)} \in \omega_{\mathrm{m}}$; and w_i is the IDW weight of the corresponding pixel $I_{(x_i y_i)}$.

4 Results and discussions

The proposed SMB filtering strategy was applied to the well-known NASA/JPL AIRSAR L-band polarimetric data of San Francisco to illustrate and verify its effectiveness. The experimental PolSAR data were originally four-look processed by averaging the Stokes matrix, and the image size is 1024×900 pixels with a pixel spacing of approximately 10 m. Figures 2(a) and (b) show the original PolSAR image and the corresponding optical image from Google Earth, respectively. The major land-cover types of the image contain heterogeneous targets, such as oriented building blocks in various directions, vegetation and two parks in the middle of the image.

4.1 Speckle reduction

To show the effectiveness of the improved SMB filter for speckle reduction, we compared the filtered SPAN (total power) data sets that were derived using the improved SMB filter, Lee's SMB filter and a 5×5 boxcar filter. For better visualization, a small area in the image center (labeled as Patch A in Fig. 2) was extracted for evaluation. The original SPAN image is shown in Fig. 3(a), which shows a serious speckle noise effect.

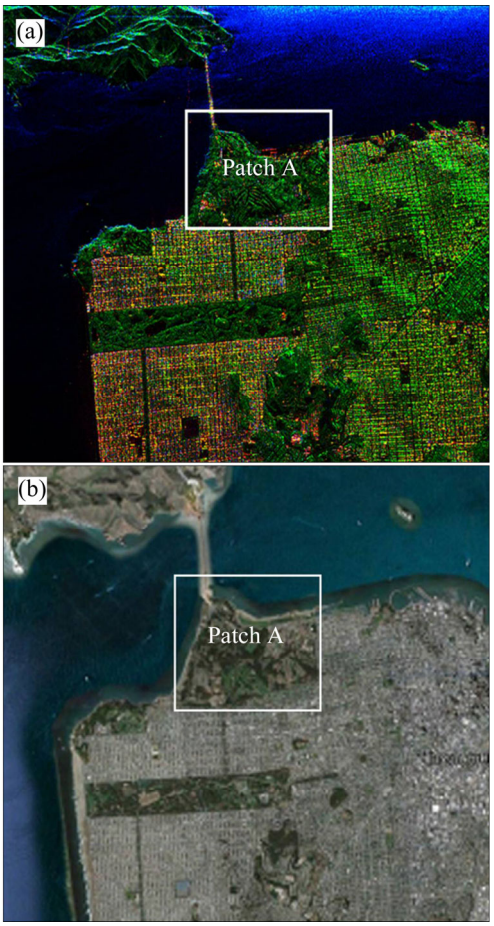

Fig. 2 Original Freeman-Durden decomposition image and corresponding optical image of San Francisco: (a) Original color-coded Freeman-Durden decomposition image (double-bounce scattering: red; volume scattering: green; surface scattering: blue); (b) Corresponding optical image from Google Earth

The filtered SPAN result of the 5×5 boxcar filter is shown in Fig. 3(b), which displays a severe loss of spatial resolution because of the overall blurring problem. The bright targets and linear features are perfectly preserved in Lee's SMB filter (Fig. 3(c)); however, some speckle noise remains in distributed areas, particularly in the grass area (e.g., the area of white circle in this figure). As shown in Fig. 3(d), the improved filter has comparable performance with Lee's SMB filter in preserving the bright media and linear features, but the speckle reduction for the distributed media is significantly improved because a more robust selection method of homogenous pixels based on the spatial majority rule was applied in the proposed speckle filter.

We also quantitatively assessed the effectiveness by calculating the equivalent number of looks (ENL) of the SPAN image, which is a common method to estimate the speckle noise level in a SAR image [20−21]. The ENL value is a widely used ratio, which is represented by μ_i^2/σ_i^2, where μ_i is the mean value, and σ_i is the

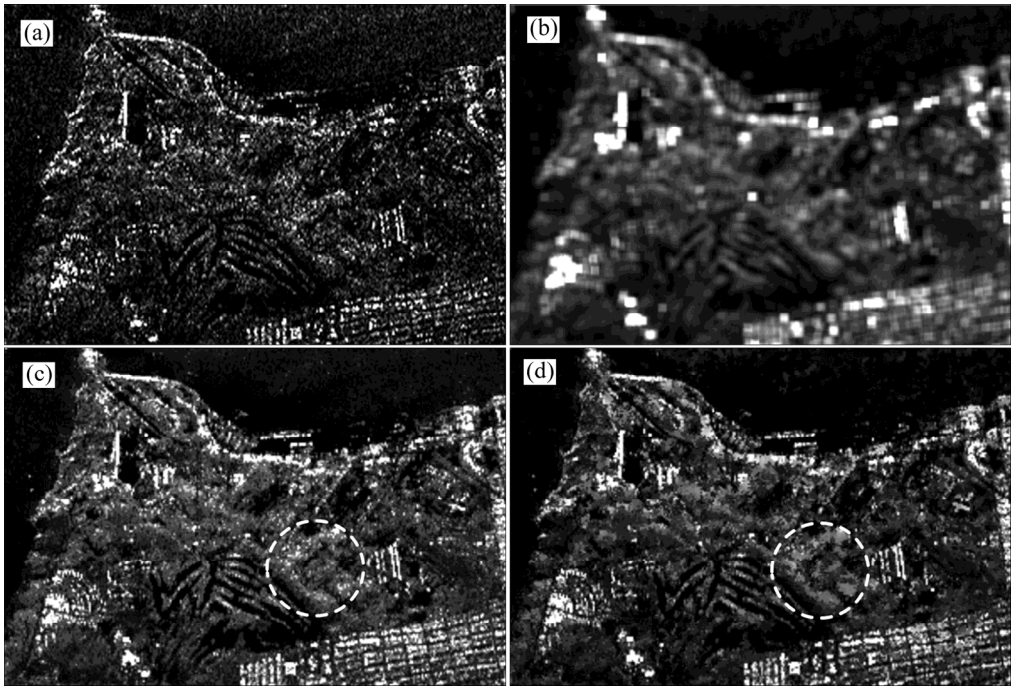

Fig. 3 Comparison of speckle reduction performance: (a) Original SPAN image; (b) 5×5 boxcar filter; (c) Lee's SMB filter; (d) Improved SMB filter

standard deviation. We calculated the ENL values for three selected typical land covers that corresponded to water body, grass and urban areas. Table 1 shows the ENL values of the original SPAN image and these three speckle filters.

Table 1 ENL values of original SPAN image and three filtered results

Area	Original SPAN image	Boxcar filter	Lee's SMB filter	Improved SMB filter
Water body	2.6287	24.4736	13.2459	23.3478
Grass area	2.2231	16.1998	8.2807	13.4105
Urban area	1.2609	6.5245	1.9281	2.079

Table 1 shows that the 5×5 boxcar filter obtained the highest ENL values for all specific types of targets. However, this result cannot imply that the boxcar filter has the best speckle filtering because the ENL carries no information of resolution degradation as illustrated in Fig. 3(b). As expected, the results of the improved SMB filter have comparable ENLs for the distributed targets (water body and grass area) with the boxcar filter, but they are largely higher than those of Lee's SMB filter. This result indicates that the improved SMB filter surpasses Lee's SMB filter in speckle reduction of homogenous areas. Furthermore, in relatively heterogeneous urban areas, both SMB filters have nearly equal and slightly larger ENLs than the unfiltered SPAN image, which indicates that both SMB filters can preserve fine-structure targets by including only pixels of identical dominant scattering mechanisms in the filtering process.

4.2 Scattering property preservation

To demonstrate the preservation of dominant scattering properties after filtering, we compared the Freeman-Durden decomposition results that were generated using the previous three speckle filters. The original color-coded Freeman-Durden decomposition image of the test site is shown in Fig. 2(a). The RGB images of the Freeman-Durden decomposition by filtering are shown in Fig. 4. As expected, the filtered decomposition result using the 5×5 boxcar filter displays the typical blurring characteristics (Fig. 4(a)), whereas Lee's SMB filter and our SMB filter have a considerable improvement in both fine-detail preservation and speckle reduction (Figs. 4(b) and (c)).

Figure 4 shows that forest and vegetation areas (illustrated in Fig. 2(b)) were correctly decomposed as volume-scattering objects (green color) in all filtered results. However, the urban areas in the right half of Figs. 4(a) and (b), particularly the oriented urban blocks that are enclosed in the white rectangles (labeled as Patch B), appear green; hence, they were misinterpreted as having volume-scattering mechanisms. These "green" urban areas in Figs. 4(a) and (b) were decomposed into red or close to red in Fig. 4(c), which indicates that double-bounce scattering is dominant. However, the

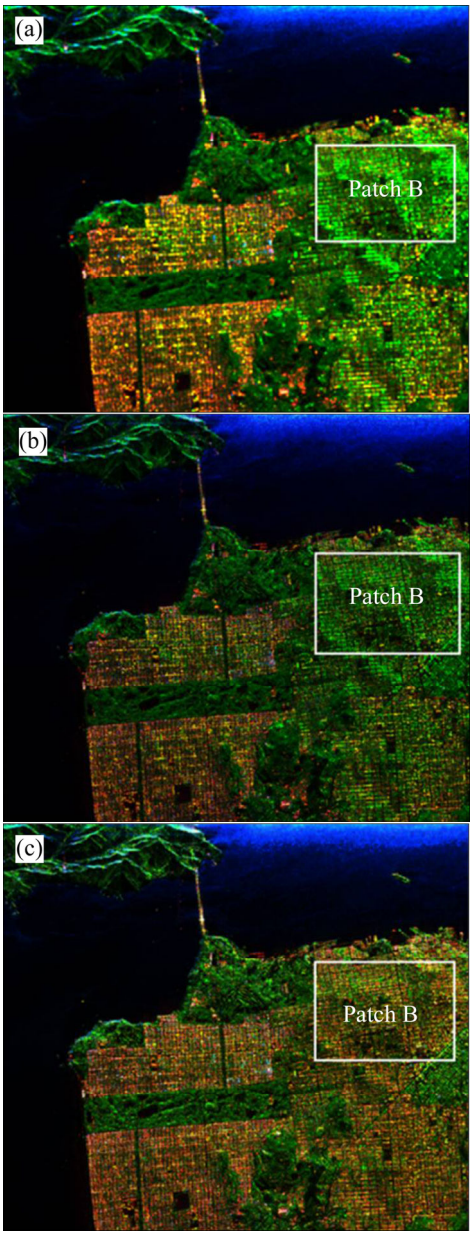

Fig. 4 Comparison of Freeman-Durden decomposition images that were filtered using: (a) 5×5 boxcar filter; (b) Lee's SMB filter; (c) Improved SMB filter (The RGB images are color-coded: red for double-bounce scattering, blue for surface scattering, and green for volume scattering)

"red" or "yellow" urban blocks in the lower right and left half parts of the image in Figs. 4(a) and (b) were enhanced in the decomposition results after the improved SMB filtering because their directions are almost orthogonal to the radar illumination. Consequently, the improved SMB filter yielded the most appropriate interpretation result of being consistent with their scattering mechanisms, which was attributed to using the new OA compensation scheme in this filter.

Furthermore, for a quantitative assessment, we counted the number of pixels that belong to three scattering mechanism categories in the decomposition results after filtering. Figure 5 shows the statistical distributions in Patch B. Figure 5 clearly shows that volume scattering is dominant in both decomposition results of the boxcar filter and Lee's SMB filter. However, in the improved SMB filter, the volume-scattering power remarkably decreases, and the surface and double-bounce scattering powers increase accordingly. Because Patch B consists of oriented urban blocks, the OA compensation procedure considerably improves the performance of the preserving scattering properties.

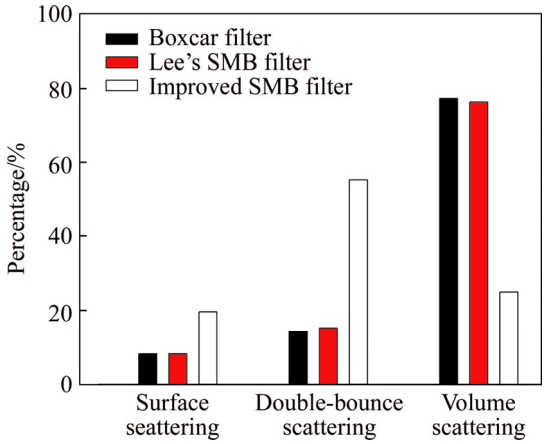

Fig. 5 Statistics of three scattering mechanism categories in Patch B for three speckle filters

5 Conclusions

The problem of Lee's SMB speckle filtering generally consists of homogenous-pixel selection and scattering property interpretation when applying the Freeman-Durden composition. In this work, an improved approach is developed by implementing the orientation angle compensation of the coherency matrix and the homogenous-pixel selection based on the spatial majority rule. By minimizing the cross-polarized component, the rotation angle is retrieved and compensated before the Freeman-Durden decomposition to remedy the overestimation of the volume-scattering contribution and improve the reliability when we select pixels of similar scattering properties in the filtering process. The spatial majority rule is used in filtering to alleviate the effect of decomposition and classification errors on the homogenous-pixel selection. This method considerably improves the speckle reduction in distributed media, particularly for high speckle noise levels. The effectiveness of the proposed approach is demonstrated using NASA/JPL AIRSAR data.

References

[1] BROWN W M. Synthetic aperture radar [J]. IEEE Trans Aerosp Electron Syst, 1967, 3: 217−229.

[2] SABRY R, VACHON P W. A unified framework for general compact and quad polarimetric SAR data and imagery analysis [J]. IEEE Trans Geosci Remote Sens, 2014, 52: 582−602.

[3] NOVAK L M, BURL M C. Optimal speckle reduction in polarimetric SAR imagery [J]. IEEE Trans Aerosp Electron Syst, 1990, 26: 293−305.

[4] LEE J S, GRUNES M R, MANGO S A. Speckle reduction in multipolarization, multifrequency SAR imagery [J]. IEEE Trans Geosci Remote Sens, 1991, 29: 535−544.

[5] GOZE S, LOPES A. A MMSE speckle filter for full resolution SAR polarimetric data [J]. J Electromagn Waves Appl, 1993, 7: 717−737.

[6] LEE J S, GRUNES M R, GRANDI G. Polarimetric SAR speckle filtering and its implication for classification [J]. IEEE Trans Geosci Remote Sens, 1999, 37: 2363−2373.

[7] GU Jing, YANG Jian, ZHANG Hao, PENG Ying-ning, WANG Chao, ZHANG Hong. Speckle filtering in polarimetric SAR data based on the subspace decomposition [J]. IEEE Trans Geosci Remote Sens, 2004, 42: 1635−1641.

[8] VASILE G, OVARLEZ J P, PASCAL F, TISON C. Coherency matrix estimation of heterogeneous clutter in high-resolution polarimetric SAR images [J]. IEEE Trans Geosci Remote Sens, 2010, 48: 1809−1826.

[9] CHEN Jiong, CHEN Yi-lun, AN Wen-tao, CUI Yi, YANG Jian. Nonlocal filtering for polarimetric SAR data: A pretest approach [J]. IEEE Trans Geosci Remote Sens, 2011, 49: 1744−1754.

[10] LEE J S, GRUNES M R, SCHULER D L, POTTIER E, FERRO-FAMIL L. Scattering-model-based speckle filtering of polarimetric SAR data [J]. IEEE Trans Geosci Remote Sens, 2006, 44: 176−187.

[11] LI Hong-zhong, CHEN Jin-song, JIANG Li-ming, LIU Lin. Preservation of polarimetric properties filtering for TSX data based on Barnes decomposition [J]. IEEE J Sel Top Appl Earth Obs Remote Sens, 2012, 5: 1831−1836.

[12] LEE J S, GRUNES M R, POTTIER E, FERRO-FAMIL L. Unsupervised terrain classification preserving polarimetric scattering characteristics [J]. IEEE Trans Geosci Remote Sens, 2004, 42: 722−731.

[13] LIAO Ming-sheng, WANG Yong, WANG Chang-cheng, LIU Lin. Modification of a scattering model-based speckle filter applied to coastal environments: An LULC study using PALSAR data [J]. Int J Remote Sens, 2010, 31: 2101−2107.

[14] KHARBOUCHE S, CLAVET D. Speckle reducing in PolSAR images for topographic feature extraction [J]. Int J Image Data Fusion, 2013, 4: 146−158.

[15] LANDGREBE D A. The development of a spectral-spatial classifier for earth observational data [J]. Pattern Recognit, 1980, 12: 165−175.

[16] YAMAGUCHI Y, MORIYAMA T, ISHIDO M, YAMADA H. Four-component scattering model for polarimetric SAR image decomposition [J]. IEEE Trans Geosci Remote Sens, 2005, 43: 1699−1706.

[17] XU Feng, JIN Ya-qiu. Deorientation theory of polarimetric scattering targets and application to terrain surface classification [J]. IEEE Trans Geosci Remote Sens, 2005, 43: 2351−2364.

[18] LAM L, SUEN S. Application of majority voting to pattern recognition: an analysis of its behavior and performance [J]. IEEE Trans Syst Man Cybern A Syst Hum, 1997, 27: 553−568.

[19] TARABALKA Y, BENEDIKTSSON J A, CHANUSSOT J. Spectral-spatial classification of hyperspectral imagery based on partitional clustering techniques [J]. IEEE Trans Geosci Remote Sens, 2009, 47: 2973−2987.

[20] TOUTZI R. A review of speckle filtering in the context of estimation theory [J]. IEEE Trans Geosci Remote Sens, 2002, 40: 2392−2404.

[21] LEE J S, WEN J H, AINSWORTH T, CHEN K S, CHEN Abel. Improved sigma filter for speckle filtering of SAR imagery [J]. IEEE Trans Geosci Remote Sens, 2009, 47: 202−213.

(Edited by YANG Hua)